A Study of the Method of Synthesis and Chromatic Properties of the Cr-SnO_2 Pigment

Beatriz Julián,[a] Héctor Beltrán,[a] Eloisa Cordoncillo,[a] Purificación Escribano,*[a] José Vicente Folgado,[b] Maria Vallet-Regí,[c] and Rafael P. del Real[c]

Keywords: Ceramics / Chromium / Chromium-tin pigment / Solid-state reactions / Tin

Chromium-doped tin dioxide has long been used as a violet pigment in the ceramic industry. However, traditional ceramic synthesis involves slow diffusion processes, high processing temperatures and serious environmental problems due to the use of carcinogenic Cr^{VI} precursors. This paper addresses the synthesis of Cr-SnO_2 by a novel, wet route that uses $Cr(acac)_3$ and $Sn(OiPr)_4$ as raw materials. The new wet method does not require handling of Cr^{VI} reagents and allows a reduction in the heat-treatment temperature from 1400 to 800 °C, which are promising economic and environmental improvements. The coloring mechanism in this pigment, currently the subject of debate, was also studied. The results indicate that the violet color is produced by the chromium ions incorporated in the cassiterite structure (SnO_2), while the quantity of chromium exceeding the network dissolution limit gives rise to Cr_2O_3 segregation, producing a greenish color. Electron spin resonance (ESR) and magnetic measurements show that chromium ions are present in the pigment in various oxidation states, reduced chromium species such as Cr^{III} and/or Cr^{IV} being responsible for the violet color.

Introduction

Cr-doped structures have been widely studied as ceramic pigments.[1−3] The influence of the host structure in the chromium ion crystal field produces a different coloring of the solid in which it acts as a chromophore.

Tin dioxide (cassiterite) exhibits a rutile structure consisting of infinite chains of octahedral SnO_6 linked by sharing of edges and corners to form a three-dimensional framework. This lattice has attracted attention as a host lattice for the incorporation of coloring metal ions such as transition metals, and also as a sealant for the inclusion of glaze-unstable colored pigments. When chromium ions are introduced into the SnO_2 structure in low quantities, they produce a violet color, yielding a pigment classified by DCMA (Dry Colour Manufacturer's Assn.) as 11-23-5.[4]

This pigment is usually synthesized by the conventional ceramic method, involving mixture dispersion of the metal oxides in a planetary ball mill and heat treatment of the mixture at 1200−1500 °C for a solid-state reaction. This procedure presents some drawbacks. Since the product formation rate is controlled by slow diffusion processes,[5] high reaction temperatures are required, with the energy costs entailed. These high temperatures produce losses of volatile reagents and hence departure from starting system stoichiometric conditions. To improve these interdiffusion processes, small quantities of various additives (mineralizers) need to be introduced. These mineralizers often contain toxic components. Furthermore, the Cr^{VI} precursors[6−9] used in Cr^{III} synthesis or oxidation to more oxidized species during heat treatment are highly toxic carcinogens.

To avoid the above disadvantages of the traditional ceramic method, a new method of synthesis for obtaining the reaction mixture has been tested. In this method the reagents are dissolved and begin to react at very low temperatures (70 °C). This synthesis route provides a high degree of homogeneity and low particle size, raising diffusion process efficiency, reducing heat-treatment temperature and avoiding the use of toxic mineralizers.

The Cr-SnO_2 pigment is an economically important material with a long history in the ceramic industry. However, its coloring mechanism is essentially unknown and a subject of debate.[9] The main difficulty could be related to determination of the oxidation states of the chromium ions in the network. Thus, little information on Cr-doped tin(IV) oxide materials is available.

[a] Departamento de Química Inorgánica y Orgánica, Universitat Jaume I
Campus Riu Sec, 12071 Castellón de la Plana, Spain
Fax: (internat.) + 34-964/728214
E-mail: escriban@qio.uji.es
[b] Institut de Ciència de Materials, Universitat de València
46071 Paterna (Valencia), Spain
[c] Departamento de Química Inorgánica y Bioinorgánica, Facultad de Farmacia, Universidad Complutense de Madrid, 28040 Madrid, Spain

To attempt to clarify some of these aspects, a study was undertaken, (i) to determine the optimum chromium content in the structure that yields the best color development by the traditional ceramic method, (ii) to design a new method of synthesis to reduce thermal treatment, and (iii) to determine the chromium oxidation states responsible for the violet color.

Results and Discussion

A preliminary study was carried out on five samples synthesized by the ceramic method (Method 1, see Table 5) to determine the relation between chromium starting quantity in synthesis and the resulting color after heat treatment. Phase evolution in the 1000−1400 °C range was studied by X-ray diffraction (XRD). Figure 1 shows the evolution of the crystalline phases for sample SC2.

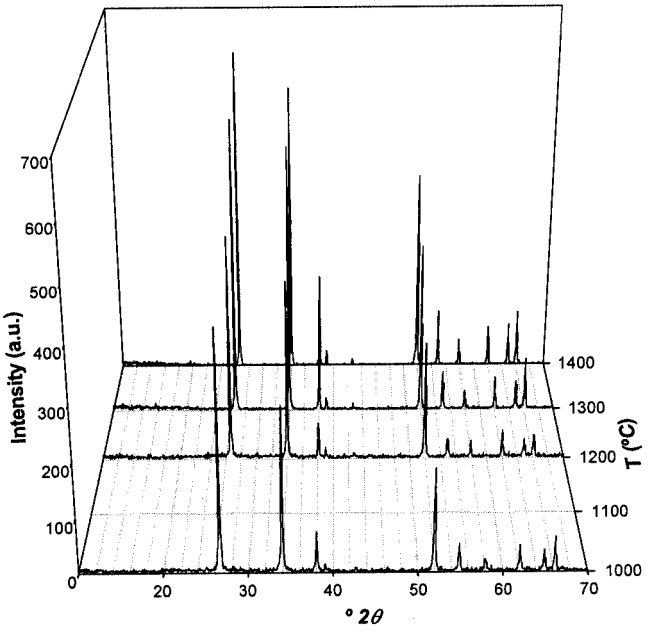

Figure 1. XRD diffractograms of sample SC2 after heat treatment at 1000, 1200, 1300 and 1400 °C for 6 h

SnO_2 (cassiterite) is the major phase in all the samples, the crystallinity of which increases with temperature. Some of the samples also exhibit peaks attributable to Cr_2O_3. The tin dioxide phase content in each sample was approximately estimated from the cassiterite (110) and Cr_2O_3 (012) peak intensities (JCPDS patterns no. 41-1445 and 38-1479, respectively) from Equation (1).

$$\%_{SnO_2} = \frac{I_{SnO_2}}{I_{SnO_2} + I_{Cr_2O_3}} \text{x}100 \quad (1)$$

Of course, for accurate analysis, a calibration curve is required for this method. XRD analysis showed a single SnO_2 phase for compositions SC1 and SC2 at all temperatures, while Cr_2O_3 was also detected for compositions SC3−SC5. In these last samples, the chromium(III) oxide phase content decreased when the temperature increased. Figure 2 plots these results. It shows that, in the samples in which the chromium content rises, high temperatures are required to produce a single phase, 1200 °C for sample SC3, 1300 °C for sample SC4, etc.

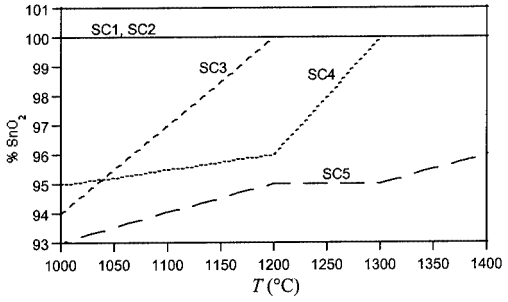

Figure 2. SnO_2 content (%) versus temperature for samples SC1, SC2, SC3, SC4 and SC5

Table 1. Colours of the samples produced by the dry method after heat treatment

Sample	1000 °C/6 h	1200 °C/6 h	1300 °C/6 h	1400 °C/6 h
SC1	pale pink	pale pink	pink-violet	violet
SC2	pale pink	pink	violet	intense violet
SC3	grey	pink-grey	pink-grey	violet-grey
SC4	grey-green	grey-pink	grey-pink	grey-pink
SC5	green	grey-green	grey-green	grey-green

Table 1 details the color of the ceramic samples heat-treated at different temperatures. For compositions with chromium contents lower than that in SC3, the violet color develops after heat treatment at 1300−1400 °C for 6 h, the SC2 composition having the most intense color. However, in samples with a chromium quantity exceeding that in SC2, a greenish shade overlies the characteristic violet color, giving rise to a greyish color for compositions SC3 and SC4, and greenish colors for SC5 at all temperatures.

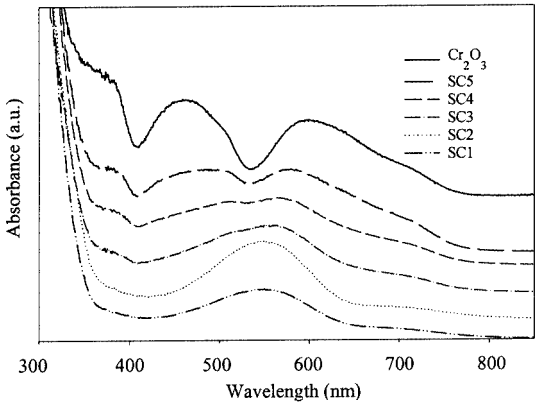

Figure 3. Diffuse reflectance spectra of ceramic samples calcined at 1400 °C for 6 h and of Cr_2O_3

Figure 3 depicts the diffuse reflectance spectra of the ceramic samples after calcination at 1400 °C for 6 h, showing the evolution of the bands with chromium content (from SC1 to SC5). The Cr_2O_3 spectrum is also included as a

reference. It is to be noted that the color of pure chromium(III) oxide is green.

In the Cr_2O_3 spectrum, two bands at 460 and 600 nm can be observed. The Cr^{III} ion, with a $3d^3$ electronic configuration, tends to an octahedral coordination. According to the Tanabe-Sugano diagram these bands can be attributed to $^4A_{2g} \rightarrow {}^4T_{2g}$ and $^4A_{2g} \rightarrow {}^4T_{1g}(F)$ spin-allowed transitions, respectively. SC1 and SC2 sample spectra exhibit a wide absorption band centerd at 18182 cm^{-1} (550 nm) and a shoulder at 14286 cm^{-1} (700 nm). In the samples with higher Cr content, however, a progressive twofold splitting of the wide absorption band can be seen. Thus, as sample SC2 developed the most intense color, the violet shade can be associated with absorption at 550 nm.

The above results indicate that, under the working conditions used, SC2 is the optimum composition. A doping ion quantity higher than that contained in $Sn_{0.985}Cr_{0.02}O_2$ cannot be fully accommodated by the host lattice, resulting in Cr_2O_3 segregation (detected by XRD), causing the greenish shade in the pigment.

It is difficult to establish where and how the chromium ion is located in the pigment, due especially to the small doping content in the violet samples (SC1 and SC2). The fact that XRD spectra of these samples detected a single tin dioxide phase at all temperatures could suggest the formation of a solid solution.

From a review of the experimental results on alloy formation, it is suggested that a difference of 15% in the radii of the metal atoms that are replacing each other is the most that can be tolerated if a substantial solid solution range is to be formed. For solid solutions in nonmetallic systems, the limiting acceptable difference in size appears to be rather larger than 15%, although difficult to quantify because it is difficult to quantify the sizes of the ions themselves.[10]

If a solid solution were formed in this system, a shift in the SnO_2 diffraction peaks should be detected, because the idealized cation radii of chromium(III) and tin(IV) ions in octahedral coordination are 75.5 and 83 pm, respectively.[11] However, comparison of XRD spectra of doped and undoped tin dioxide showed no deviations in peak positions. On the other hand, if there is free Cr_2O_3 outside the tin dioxide lattice, the amount must be below the sensitivity threshold of the instrument. XRD analysis therefore does not enable solid solution formation to be established.

The Cr-SnO_2 pigment composition was thus optimized (sample SC2) by the ceramic method. This composition was therefore prepared by the wet method (sample referenced SC6). Undoped tin dioxide was also synthesized as a reference under the same conditions (sample S2).

XRD characterization of the powders produced by Method 2 (after heating under reflux and evaporation of the solvent) showed that they were amorphous. To determine the cassiterite crystallization temperature and to design an appropriate heat treatment to remove organic matter, differential thermal (DTA) and thermogravimetric (TG) analyses were performed. Figure 4 shows the DTA/TG data for sample SC6 in the 25−1200 °C range.

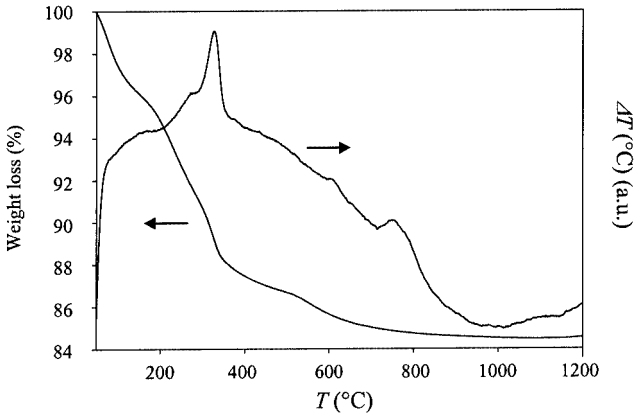

Figure 4. DTA/TG curves found for sample SC6

The DTA curve of SC6 displayed several broad exothermic peaks below 650 °C, which were accompanied by a gradual weight loss of 15% as detected by TG measurements. These bands can be assigned to solvent evaporation (below 150 °C) and decomposition/combustion of the organic groups. An exothermic peak without weight loss at 750 °C was also detected. This latter peak could be tentatively associated with cassiterite crystallization. To confirm this, the sample was heat-treated at several temperatures below and above 750 °C, followed by XRD analysis. The resulting XRD patterns indicated that SnO_2 crystallization occurred at 400 °C. The crystallization peak in the DTA curve is probably overlapped by organic matter burnout (between 150 and 650 °C) and cannot be detected. Moreover, the same peak was also observed in the undoped sample (SC2). This exothermic peak was therefore associated with SnO_2 phase transformation.

In spite of the detection of SnO_2 crystallization at 400 °C, heat-treatment design needed to ensure complete removal of organic matter. Taking this into account and also to enable comparison of the results of the two methods of synthesis, the following heat-treatment schedule was adopted. Samples SC2 and SC6 (with the same composition but synthesized by different methods) were calcined in air at a heating rate of 10 °C/min at 800, 1000, 1200, 1300, and 1400 °C for 6 h, with a hold at 500 °C for 1 h. The diffractograms of the samples indicate the presence of SnO_2 as single phase, while the diffraction peak intensity increases with temperature.

Table 2 shows the color and CIELAB (L*a*b*) parameters of samples SC2 and SC6 after heat treatment at several temperatures.

In Table 2 the same color evolution can be observed for both samples from 1000 to 1400 °C. However, at 800 °C the ceramic sample exhibited a yellow color, whereas sample SC6 exhibited a violet color with L*a*b* parameters similar to those found for the SC2 sample after calcination at 1400 °C for 6 h. The wet method thus reduced the synthesis temperature by 600 °C.

The diffuse reflectance spectra of the SC2 and SC6 samples under different heat-treatment conditions are dis-

Table 2. L* a* b* parameters for SC2 and SC6 samples heat treated at different temperatures

	800 °C/6 h		1000 °C/6 h		1200 °C/6 h		1400 °C/6 h	
Sample	SC2	SC6	SC2	SC6	SC2	SC6	SC2	SC6
Color	yellow	violet	pale pink	pale pink	pink	pink	violet	intense violet
L*	79.83	61.06	83.66	78.26	82.10	83.61	63.28	50.83
a*	2.15	15.95	3.71	6.65	4.63	3.89	15.33	15.92
b*	7.26	−12.48	2.71	2.01	1.16	4.49	−12.08	−12.74

played in Figure 5, part a) (ceramic method) and part b) (dissolution method).

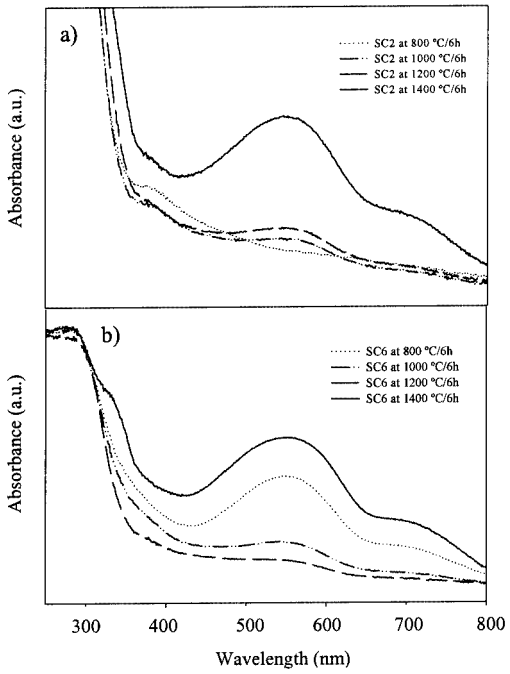

Figure 5. Diffuse reflectance spectra of samples (a) SC2 and (b) SC6 heat-treated at 800, 1000, 1200 and 1400 °C for 6 h

All the spectra show a strong absorption band in the ultraviolet zone (from 200 to around 350 nm) but different behavior is observed in the two synthesis methods. The most remarkable fact is the similarity between the spectra of the SC2 sample, calcined at 1400 °C for 6 h, and the SC6 sample calcined at 800 °C for 6 h, producing the same color in the two samples (Table 2). The spectrum of sample SC6 heat treated at 1400 °C shows a high intensity for the band centerd at 550 nm, which explains the very intense violet color exhibited by this sample.

Although exhaustive study for thorough understanding of the pigment-coloring mechanism is still pending, exploratory studies were performed to determine the origin of the differences found in the colors of samples SC2 and SC6 heat-treated under the same conditions.

The first explanation advanced was that the violet color was related to the quantity of chromium introduced into the SnO_2 framework. This would allow a ready explanation of the violet color found in the sample prepared by the wet method at 800 °C, since the degree of homogeneity and the reaction rate are much higher than in the ceramic method.

An estimation was therefore made of the Cr content inside and outside the framework for the SC2 and SC6 samples calcined at 800 and 1200 °C for 6 h. These two temperatures were chosen because at 800 °C/6 h the colors of the two samples were quite different, while at 1200 °C/6 h the color was the same. The samples were washed by the procedure described in the Exp. Sect. Acid attack and oxidation to Cr^{VI} were performed to remove the unretained chromium in the SnO_2 lattice. The Cr^{VI} content in the washing liquids was determined by atomic absorption spectrometry (AAS), and the Cr content in the washed powders was analysed by X-ray fluorescence (XRF). The values, expressed in mol Cr/g pigment, are summarized in Table 3.

Table 3. Cr^{VI} content in washing liquids and Cr content in washed powders

Sample	800 °C/6 h	1200 °C/6 h
SC2 (washing liquids)	3.034×10^{-5}	1.283×10^{-5}
SC2 (powders)	1.171×10^{-4}	1.355×10^{-4}
SC6 (washing liquids)	2.657×10^{-5}	1.794×10^{-5}
SC6 (powders)	1.118×10^{-4}	1.013×10^{-4}

The initial chromium content was 1.334×10^{-4} mol/g pigment. Table 3 shows that the Cr^{VI} content in the washing liquids is slightly higher in samples heat-treated at 800 °C for 6 h. This is a reasonable finding, if it is taken into account that the introduction of chromium into the SnO_2 structure requires slow diffusion processes, which improve with increasing temperature. However, no significant difference in Cr^{VI} content, that could be responsible for the drastic difference in color (at 800 °C), was found between the washing liquids of samples SC2 and SC6. Moreover, the color of the washed and unwashed samples does not differ significantly. On the other hand, the Cr content detected in the solid by XRF for both samples at the two temperatures is also similar (it is to be noted that measurement was at the detection limit of this technique).

Due to the similarity of the Cr content in both samples, the differences in color can be considered mainly due to variations in the oxidation state of the chromium ions, and not to the chromium content introduced into the SnO_2 structure.

In order to analyse the chromium oxidation states, electron spin resonance (ESR) analysis was performed for samples SC2 and SC6 heat-treated at 800 and 1200 °C. The ESR spectra found are depicted in Figure 6.

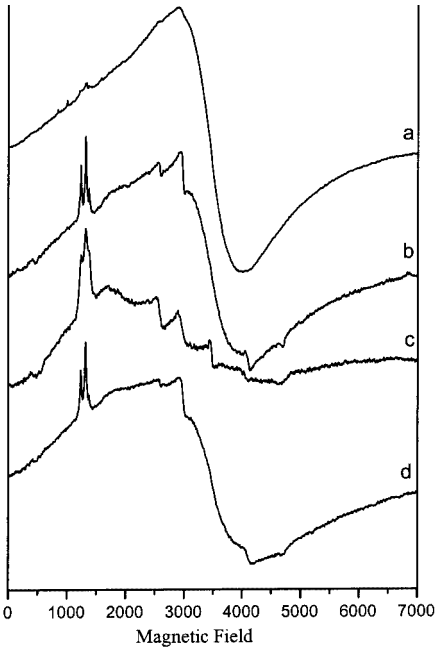

Figure 6. ESR spectra of sample SC2 heat-treated at 800 °C/6 h (a) and 1200 °C/6 h (b), and sample SC6 heat-treated at 800 °C/6 h (c) and 1200 °C/6 h (d)

The four spectra are each dominated by a very broad signal centerd at a g value of ca. 2, with other, narrower, superimposed peaks. The ratio between the narrow and the broad signals depends on the method of synthesis and the heat-treatment temperature. These facts indicate the presence of Cr^{3+} in the samples. The broad isotropic signal can be attributed to Cr_2O_3-like clusters, whereas the narrow signals correspond to isolated Cr^{3+} ions (i.e., diluted in a diamagnetic lattice[12−14]). Broad signals at $g = 2$ have also been observed in mixed-valence trimers of the type $Cr^{VI}-O-Cr^{III}-O-Cr^{VI}$ with an average oxidation state of +5.[15,16]

The spectra of sample SC2 at 800 °C/6 h are dominated by the signal at $g = 2$, indicating that the chromium ions are predominantly forming clusters. In contrast, for sample SC6 at the same temperature, the chromium ions basically appear as isolated species and the relative quantity of clusters is smaller. Moreover, in the latter sample, a very weak sharp signal at $g = 2$ may indicate the presence of a small quantity of Cr^{V} or tetrahedrally coordinated Cr^{IV} ions.[17] Almost identical spectra were found for the SC2 and SC6 samples heat-treated at 1200 °C for 6 h. In these samples, isolated Cr^{3+} ions and clusters are observed and, although the cluster fraction is still significant, it is lower than that in SC2 at 800 °C for 6 h.

With regard to the set of signals associated with isolated Cr^{3+} ions, at least seven features are observed in each spectrum. Careful study of these signals indicates that they are due to the presence of Cr^{3+} in two different polyhedral coordinations, both corresponding to orthorhombically distorted octahedra.[12−14] Cr^{III} is an $S = 3/2$ ion and exhibits a zero field splitting (characterized by D and E parameters), which is very sensitive to small variations of the local crystal field. In our case, the spectra are typical of $2D >> h\nu$ and $E \neq 0$, and two groups of five signals should be expected under the experimental conditions used. Although no accurate calculations can be performed, due to overlapping and poor resolution of the signals, a value of $D > 0.6$ cm^{-1} and an E/D ratio of ca. 0.22 and 0.28 can be estimated for the two slightly different sites. The higher E value corresponds to a major orthorhombic distortion of the site. These values are very similar to those found in Cr^{3+} diluted in TiO_2-rutile,[12−14] and suggest that Cr^{3+} is incorporated into the Sn sites in the SnO_2 lattice.

This study reflects the tendency of paramagnetic chromium ions to form clusters with strong Cr−Cr interactions. Since no remarkable differences in chromium oxidation states were found in the different samples and no clear signal associated with isolated Cr^{V} species and Cr^{IV} ions was detected, the color difference could be related to the quantity of chromium in each oxidation state. The clustering effect may modify the color slightly, but would not be expected to produce the drastic changes in color found in these samples.

To confirm the presence of Cr^{III} in the two different distorted octahedral environments, the band observed in the UV/Vis spectra at 550 nm was deconvoluted by a Gaussian function. Figure 7 shows that this band can be resolved into two bands centerd at 578 and 510 nm, which matches ESR results.

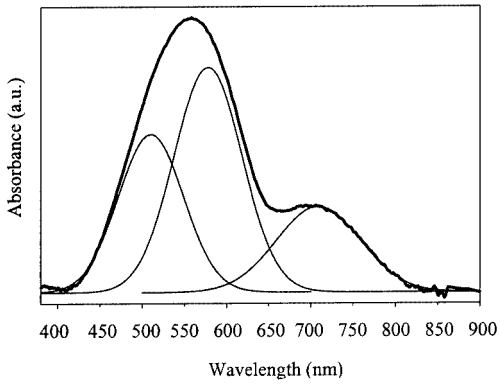

Figure 7. Deconvolution in Gaussian functions of the band centerd at 550 nm

According to the Tanabe-Sugano diagram, two other bands should be observed in the UV/Vis region. The most energetic band should appear in the UV zone and cannot be detected. The second band associated with a $^4A_{2g} \rightarrow {}^4T_{2g}$ transition should appear at around 380 nm, but is overlapped by a broad charge-transfer band in the UV zone.

The presence of Cr^{IV} ions was also studied in the absorption spectra, but no characteristic signals of this species were found (in the IR region, at 1000−1200 nm).[18] If any Cr^{IV} ions are contained in the pigment, they must be in

small quantities as they are not detected within the sensitivity limits of the instrument.

As the presence of Cr^{II} ions was precluded under the synthesis conditions used, the existence of chromium ions in more than one oxidation state (Cr^{VI}, Cr^{V}, Cr^{IV} and Cr^{III}) was determined from measurements of magnetic moment (*m*) vs. magnetic field (*H*) at a constant temperature of 77 K. For this purpose the magnetic response of a sample is assumed to be generated from the paramagnetic contributions of the chromium ions in each oxidation state. It was further assumed that the chromium ions in a sample are only contained in two oxidation states, Cr^{VI} (with no magnetic response) and Cr in another oxidation state (III, IV or V, each having its own magnetic response). Table 4 summarizes the calculated quantity of Cr^{VI} contained in the structure for each pair of oxidation states (Cr^{III} and Cr^{VI}, Cr^{IV} and Cr^{VI}, or Cr^{V} and Cr^{VI}).

Table 4. Cr^{VI} content (%) in the samples for each pair of oxidation states

	Cr^{VI} (%)			
Oxidation state	SC2 at 800 °C/6 h	SC6 at 800 °C/6 h	SC2 at 1200 °C/6 h	SC6 at 1200 °C/6 h
Cr^{III}	82	40	91	81
Cr^{IV}	66	0	84	64
Cr^{V}	8	−	57	5

The Cr^{VI} content (%) was found from the slope (*m* vs. *H*) and quantity of Cr in the samples.[19]

The data indicate that all samples contain chromium ions in different oxidation states. Sample SC6 at 800 °C shows a high magnetic response, which could be attributable to all the chromium ions being in oxidation state IV (and no Cr^{VI} would be present). However, since Cr^{III} was detected by ESR, it must also contain Cr^{VI}, so that this sample must mainly contain species in low oxidation states (Cr^{III} and Cr^{IV}) and a minor quantity of Cr^{VI}. All the other samples show low magnetization values indicating a very high Cr^{VI} content, this being especially notable for sample SC2 at 1200 °C for 6 h. Samples SC2 at 800 °C and SC6 at 1200 °C exhibit the same magnetic behavior, but different colors. This can be explained by the assumption of a different distribution of chromium ions in the various oxidation states.

The ESR results and magnetic measurements therefore indicate that differences in color are directly related to the quantity of chromium in each different oxidation state, and must be mainly generated by reduced species such as Cr^{III} and Cr^{IV}. Emission measurements are currently under further investigation in order to achieve a better understanding of the coloring mechanism.

Conclusion

A new synthesis method to prepare chromium-doped tin dioxide from a mixture of Sn^{IV} and Cr^{III} precursors has been devised, and compared with the traditional ceramic method. The composition that developed the best violet color under the working conditions used was $Sn_{0.985}Cr_{0.02}O_2$. The great advantage of this dissolution method is that the intense violet color can be produced after heat treatment at 800 °C for 6 h, whereas the traditional method requires heat treatment at 1400 °C for 6 h. An excess of chromium content in the SnO_2 structure causes the segregation of Cr_2O_3, giving rise to a greenish shade.

ESR studies reflect the tendency of paramagnetic chromium ions to form clusters with strong Cr−Cr interactions and reveal that the main chromium oxidation state in all the samples is Cr^{III}. The presence of Cr^{IV} ions was also studied by diffuse reflectance spectra but no characteristic signals of this species were found.

All the studies performed to establish the coloring mechanism indicate that the origin of the violet color is unrelated to the quantity of chromium introduced in the structure, but is directly associated with the quantity of chromium present in different oxidation states, the reduced chromium species (Cr^{III} and/or Cr^{IV}) being mainly responsible for the violet color.

This new synthesis method presents promising results for the ceramic industry from an economic and environmental standpoint.

Experimental Section

General Remarks: Two different synthesis routes for preparing the precursor mixture for the solid-state reaction were developed, the traditional ceramic method from Sn^{IV} and Cr^{III} oxides (Method 1) and a method in which the Sn^{IV} and Cr^{III} reagents are dissolved (Method 2). The nominal compositions and references of the samples synthesized are summarized in Table 5. In a first step, the optimum Cr content was established for samples produced by the ceramic method and the best composition (SC2 sample) was also synthesized by the dissolution method (SC6 sample). In Method 1, the following precursors were used: SnO_2 (Panreac, analytical grade) and Cr_2O_3 (Merck, analytical grade). These samples were prepared by mixing and homogenizing stoichiometric amounts of each precursor in a planetary ball mill, with acetone used as a dispersant. After evaporation of the dispersant at room temperature, the samples were dried under infrared lamps. In Method 2, synthesis was performed by heating the appropriate amount of $Cr(acac)_3$ (Merck, pure grade) under reflux in a 2-propanol solution of $Sn(OiPr)_4 \cdot i$PrOH adduct (ABCR, analytical grade). Sample

Table 5. Nominal composition of the samples

Sample	Composition	Method of synthesis
SC1	$Sn_{0.992}Cr_{0.01}O_2$	1
SC2	$Sn_{0.985}Cr_{0.02}O_2$	1
SC3	$Sn_{0.956}Cr_{0.06}O_2$	1
SC4	$Sn_{0.927}Cr_{0.1}O_2$	1
SC5	$Sn_{0.86}Cr_{0.2}O_2$	1
S2	SnO_2	2
SC6	$Sn_{0.985}Cr_{0.02}O_2$	2

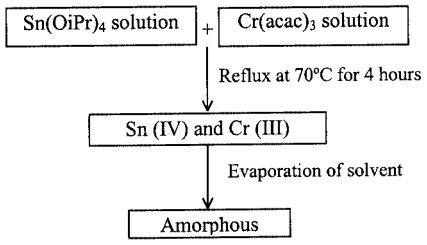

Figure 8. Synthesis diagram of S2 and SC6 samples

preparation is set out in the flow diagram in Figure 8. As an SnO_2 structure is generated during heat treatment in this method of synthesis, an undoped sample (referenced S2) was prepared by the same experimental procedure. All the samples were heat-treated in an electric furnace at different temperatures (from 800 to 1400 °C for 6 h) at a heating rate of 10 °C/min. In order to refine and homogenize the particle size after calcination, the resulting product was ground in an agate mortar with acetone, followed by sieving to 50 μm.

Instrumentation: Crystalline phase evolution of the calcined powders was monitored by X-ray powder diffraction (XRD) with a SIEMENS D5000 diffractometer with Cu-K_α radiation. Data were collected by step-scanning from $2\theta = 10$ to 70° with a step size of $2\theta = 0.050°$ and 1 s counting time per step. The automatic diffractometer was controlled by "SIEMENS DIFFRACT plus" software, which records diffraction peak positions and intensities. Differential thermal (DTA) and thermogravimetric (TG) analyses were performed in a Mettler Toledo model SDTA 851^e. All experiments were run in air from 25 to 1200 °C with a heating rate of 10 °C/min. UV/Vis spectra (diffuse reflectance) and CIELAB parameters were determined at room temperature with a spectrophotometer (CARY 500 SCAN) and a coupled analytical software for color measurements. The data were registered from 200 to 1400 nm with a PTFE blank as reflecting standard. CIELAB color parameter measurements were conducted using a D65 standard illuminant. ESR experiments were performed at 100 K with a Bruker spectrophotometer (ER200D) in the X-band at 9.5 GHz. Magnetic susceptibilities were recorded as a function of the magnetic field at 20 K with a SQUID magnetometer ($H_{max} = 5$ T). In view of the high carcinogenicity of Cr^{VI} ions, the Cr^{VI} content in the washing liquids of the samples was determined by atomic absorption. 1 g of sample was subjected to successive washings with hot 0.3 M HNO_3 until 100 mL of solution was obtained. Measurements were conducted with a Varian Spectra 640 atomic absorption spectrophotometer. Besides these analyses, the chromium content was determined on solid samples by X-ray fluorescence spectrometry with a PHILIPS instrument (Model PW 2400) fitted with an Rh tube and eight single crystals for analysis: LiF200, LiF220, GE(111), InSn, PE, TLAP, PX1 and PX3.

Acknowledgments

The financial support of the Spanish CICYT (project No. PB98-1042) is gratefully acknowledged. We thank the Spanish government for a doctoral fellowship (B. J.).

[1] S. A. Chronister, W. Chen, *Am. Ceram. Soc. Bull.* **1994**, *73*, 71−75.
[2] A. C. Airey, W. Roberts, *Ceram. Eng. Sci. Proc.* **1987**, *8*, 1168−1187.
[3] E. Cordoncillo, F. Del Rio, J. Carda, M. Llusar, P. Escribano, *J. Eur. Ceram. Soc.* **1998**, *18*, 1115−1120.
[4] *DCMA Classification and Chemical Description of the Mixed Metal Oxide Inorganic Coloured Pigments*, 2nd ed., Metal Oxides and Ceramics Colours Subcommittee, Dry Colour Manufacturer's Assn., Washington DC, **1982**.
[5] W. D. Kingery, H. K. Bowen, D. R. Uhlmann, *Introduction to Ceramics*, 2nd ed., John Wiley and Sons, New York, **1976**, p. 314.
[6] A. M. Heyns, P. M. Harden, *J. Phys. Chem. Solids* **1999**, *60*, 277−284.
[7] D. G. Park, J. M. Burlitch, R. F. Geray, R. Dieckmann, D. B. Barber, C. R. Pollock, *Chem. Mater.* **1993**, *5*, 518−524.
[8] S. Ishida, S. Kanaoka, I. Kato, M. Hayashi, *Yogyo-Kyokai-Shi* **1985**, *94*, 457−463.
[9] P. G. Harrison, N. C. Lloyd, W. Daniell, C. Bailey, W. Azelee, *Chem. Mater.* **1999**, *11*, 896−909.
[10] A. R. West, *Solid State Chemistry and its Applications*, John Wiley and Sons, New York, **1992**, p. 359.
[11] R. D. Shannon, *Acta Crystallogr., Sect. A* **1976**, *32*, 359.
[12] R. Biasi, A. Fernandes, M. Grillo, *J. Am. Ceram. Soc.* **1993**, *76*, 223−225.
[13] S. Ishida, M. Hayasi, Y. Fujimura, *J. Am. Ceram. Soc.* **1990**, *73*, 3351−3355.
[14] S. Doeuff, M. Henry, C. Sanchez, J. Livage, *J. Non-Cryst. Solids* **1987**, *89*, 84−97.
[15] P. G. Harrison, N. C. Lloyd, W. Daniell, *J. Phys. Chem. B* **1998**, *102*, 10672−10679.
[16] C. S. Sunandana, *Mater. Res. Bull.* **1985**, *20*, 531−537.
[17] P. S. Devi, H. D. Gafney, V. Petricevic, R. R. Alfano, D. He, K. E. Miyano, *Chem. Mater.* **2000**, *12*, 1378−1385.
[18] H. Eilers, U. Hommerich, S. M. Jacobsen, W. M. Yen, *Phys. Rev. B* **1994**, 15505.
[19] B. D. Cullity, *Introduction to magnetic materials*, Addison Wesley, Reading, MA, **1972**.

Received March 22, 2002
[I02150]